Phase transition and electrical properties of $(1 - x)(K_{1/2}Na_{1/2})NbO_3$–$xBi(Sc_{3/4}Co_{1/4})O_3$ lead-free ceramics

Hualei Cheng[a)]
Shaanxi Key Laboratory of Phytochemistry, Department of Chemistry, Baoji University of Arts and Science, Baoji, Shaanxi 721013, China; and State Key Laboratory of Solidification Processing, Northwestern Polytechnical University, Xi'an, Shaanxi 710072, China

Hongliang Du
State Key Laboratory of Solidification Processing, Northwestern Polytechnical University, Xi'an, Shaanxi 710072, China; and College of Science, Air Force Engineering University, Xi'an, Shaanxi 710051, China

Wancheng Zhou and Fa Luo
State Key Laboratory of Solidification Processing, Northwestern Polytechnical University, Xi'an, Shaanxi 710072, China

(Received 22 January 2015; accepted 17 July 2015)

Lead-free ceramics $(1 - x)(K_{1/2}Na_{1/2})NbO_3$–$xBi(Sc_{3/4}Co_{1/4})O_3$ [$(1 - x)$KNN–xBSC] were prepared by the conventional solid-state sintering method. X-ray diffraction patterns show that the introduction of BSC into KNN system caused insignificant change in crystal structure. The composition with $x = 0.015$ has diphasic tetragonal and orthorhombic phases. Moreover, the grain size significantly dependent on the composition. The phase transition temperatures of orthorhombic–tetragonal ($T_{O–T}$) and tetragonal–cubic (T_C) decreased with increasing x from 0 to 0.025. The $T_{O–T}$ value of KNN–0.015BSC ceramic is close to room temperature, resulting in good electrical properties ($d_{33} = 190$ pC/N, $k_p = 40.3\%$, $\varepsilon_r = 1494$, $tg\delta = 0.026$), with the Curie temperature $T_C = 321$ °C. The combination of good piezoelectric properties and high T_C makes these KNN–BSC ceramics suitable for elevated temperature piezoelectric devices.

I. INTRODUCTION

Recently, there is an urgent need for piezoelectric devices used under the extreme conditions, especially high working temperature which is higher than that of current available $Pb(Zr,Ti)O_3$ (PZT), such as space exploration, oil or gas pipeline health monitoring, automotive smart brake, and so on.[1–3] To achieve this, Eitel et al. used an experiential relationship between tolerance factors (t) of perovskite near morphotropic phase boundary (MPB) and predicted that the $BiScO_3$–$PbTiO_3$ (BS–PT) systems should have excellent piezoelectric properties with a wider range of thermal stability.[4,5] Among, BS plays an important role in enhancing piezoelectric properties and T_C. Extending the investigations of BS–PT perovskite compositions, the substitutions of Sc by the other metal ions (i.e., Fe, Sc, Co, Ga, In, etc.) have been developed and found these systems show enhanced properties and/or higher transition temperatures.[6–8] However, these systems still contain lead element. Lead brings great threat to the environmental and does harm to human health during the course of manufacturing, using and abandoning. In view of the sustainable development of the world, it is necessary to seek environmentally friendly lead-free piezoelectric materials for replacing the conventional lead-based ceramics.

Following that prediction and to develop lead-free materials with improved qualities, a lead-free analog of BS–PT has been prepared with $(K_{1/2}Na_{1/2})NbO_3$ (KNN, $t = 1.01$) to replace the PT ($t = 1.019$) and the KNN–$BiMeO_3$ (Me = Mn, Fe, Co, Al, Sc) solid solutions have been performed for the purpose of developing high T_C ceramics with piezoelectric properties.[9–17] The KNN–BS ceramics show a MPB at $0.015 \le x \le 0.02$ and the enhanced piezoelectric properties.[14] Additionally, the 0.04BS–0.96KNN ceramics show a broad and stable permittivity maximum near 1500 and dielectric loss less than 5% at 100–300 °C.[15,16] The effects of the $BiCoO_3$ addition on the phase structure, dielectric, piezoelectric, and ferroelectric properties of KNN–xBC ceramics have been systematically investigated.[17] And the improved electrical properties were induced by the polymorphic phase transition (PPT) from rhombohedral to orthorhombic phase.[17,18] Recently, the optimized piezoelectric coefficient $d_{33} > 400$ pC/N can be obtained by building up a novel MPBs between rhombohedral and tetragonal phases in KNN-based ceramics.[18–21] Introducing additives inducing rhombohedral phase, such as $BaZrO_3$

Contributing Editor: Ian M. Reaney
[a)]Address all correspondence to this author.
e-mail: hualeicheng@163.com.
DOI: 10.1557/jmr.2015.228

(Refs. 22 and 23) and Sb,[24] can increase the transitional temperature of rhombohedral and orthogonal phases (T_{R-O}), and also introducing additives inducing tetragonal phase can decrease the transitional temperature of orthorhombic and tetragonal phases (T_{O-T}).[25] The $(Bi_{0.5}Na_{0.5})ZrO_3$ (BNZ) combines the function of reducing T_{O-T} and increasing T_{R-O} in one body to achieve constructing MPB at room temperature.[26] The optimum electrical properties were obtained: d_{33} = 360 pC/N, k_p = 32.1%, ε_r = 1429, tgδ = 3.5%, and T_C = 329 °C.[26] This novel idea provides a new direction for enhancing the properties of KNN-based ceramics.

Considering that $BiCoO_3$ (t = 0.967) is similar to $BiScO_3$ (t = 0.907) in phase structure, however, there are no systematic investigations on the solid solution of $BiScO_3$–$BiCoO_3$–$(K_{1/2}Na_{1/2})NbO_3$ (BSC–KNN) ternary system ceramics till now. In addition, Co_2O_3 is an effective sintering aid for the KNN-based ceramics[27,28] and the partial substitution of Sc_2O_3 by Co_2O_3 would reduce the cost of KNN–BSC ceramics. Therefore, $Bi(Sc_{3/4}Co_{1/4})O_3$ was used as a new end member to substitute for KNN and the structural and electrical properties of the $(1-x)$ $(K_{1/2}Na_{1/2})NbO_3$–$xBi(Sc_{3/4}Co_{1/4})O_3$ ternary system were investigated. We expect to provide promising candidate materials for KNN-based ceramics with good temperature stability along with high piezoelectric properties for practical applications by this study.

II. EXPERIMENTAL PROCEDURE

K_2CO_3 (99%), Na_2CO_3 (99.8%), Nb_2O_5 (99.5%), Bi_2O_3 (99.0%), Sc_2O_3 (99.9%), and Co_2O_3 (99%) were used to prepare $(1-x)$ $(K_{1/2}Na_{1/2})NbO_3$–$xBi(Sc_{3/4}Co_{1/4})O_3$ [abbreviated as $(1-x)$KNN–xBSC, x = 0–0.025] ceramics by the conventional solid-state sintering method. To obtain the stoichiometric composition, all powders were separately dried in an oven at 110 °C for 5 h prior to mixing. The stoichiometric powders were mixed by ball-milling in alcohol for 24 h, dried and then calcined at 950 °C for 5 h. The calcined powders were ball-milled again for 12 h, dried and pressed into the disks of 12 mm in diameter and 1 mm in thickness under 300 MPa using polyvinyl alcohol (PVA) as a binder. After burning off PVA, the pellets were sintered at 1120 °C for 2 h in the sealed Al_2O_3 crucibles. The obtained samples were polished. Silver paste was fired on both sides of the samples at 810 °C for 20 min as the electrodes for the sake of measurements.

The phase structures of the sintered ceramics were examined using x-ray powder diffraction analysis with a Cu K_α radiation (Philips X-Pert ProDiffractometer, Almelo, The Netherlands) at room temperatures. The microstructure evolution was observed using a scanning electron microscopy (SEM) (model JSM-6360, JEOL, Tokyo, Japan). The dielectric spectrum measurements were performed using the LCR meter (Agilent E4980, Agilent Technologies, CA) with a heat rate of 3 °C/min in a temperature range of 0–520 °C and a frequency range of 1–1000 kHz. The piezoelectric constant d_{33} was measured using a quasi-static d_{33} meter (Model ZJ-3, Institute of Acoustics Academic Sinica). The planar electromechanical coupling factor k_p was calculated by the resonance–antiresonance method on the basis of IEEE standards using an impedance analyzer (Agilent 4294A).

III. RESULTS AND DISCUSSION

A. Structure and microstructure evolution

Figure 1 shows the x-ray diffraction (XRD) patterns of $(1-x)$KNN–xBSC ceramics at room temperature. As can be seen from Fig. 1(a), all samples show a pure perovskite phase and no secondary phase could be certified. This indicates that $Bi(Sc_{3/4}Co_{1/4})O_3$ (BSC) has completely diffused into the KNN lattice to form stable $(1-x)$KNN–xBSC solid solutions. Detailed composition-dependent XRD patterns between 2θ = 40° and 50° are enlarged in Fig. 1(b). The orthorhombic phase and tetragonal phase are characterized by (202)/(020) peak and (002)/(200) peak splitting at about 45°, respectively.[29] According to Fig. 1(b), the $(1-x)$KNN–xBSC

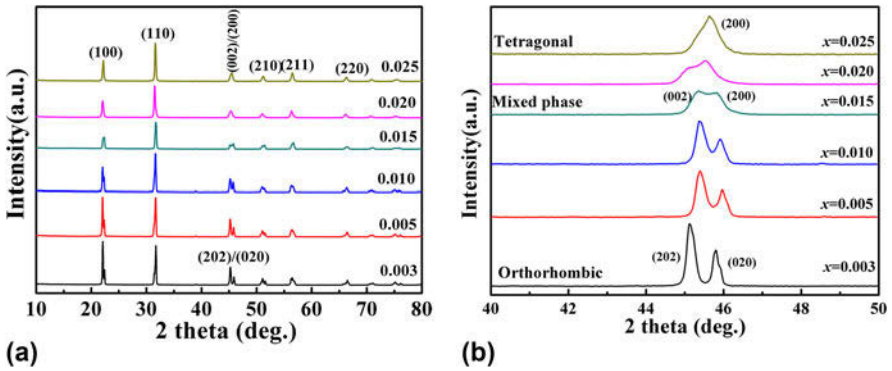

FIG. 1. (a) XRD patterns of $(1-x)$KNN–xBSC ceramics as a function of x and (b) enlarged XRD patterns between 2θ = 40° and 50°.

($x \leq 0.010$) ceramics are single perovskite phase with orthorhombic crystal system and it becomes a tetragonal perovskite structure when $x \geq 0.020$. The coexistence of orthorhombic and tetragonal phases at $x = 0.015$, namely, there is the formation of the so called MPB in the $(1 - x)$KNN–xBSC ceramics at $x = 0.015$. However, the tetragonal phase is very unstable and disappears rapidly with adding more BSC. At $x = 0.025$ approximately, the (002) peak becomes weak, indicating the formation of the pseudocubic phase. In additional, the diffraction peaks slightly shift to lower angle meaning the space distance increases gradually. This can be explained as follows: the ionic radius of Bi^{3+} (0.13 nm, CN = 12) is much larger than that of Nb^{5+} (0.064 nm, CN = 6), and Bi^{3+} may substitute for being introduced into the A site of the perovskite structure to substitute Na^+ and K^+ in KNN ceramics owing to the close ionic radius. The Sc^{3+} (0.075 nm, CN = 6) and Co^{3+} (0.055 nm, CN = 6) are introduced into the B-site owing to the small ion radius. Consequently, the addition of BSC yields a distortion of the structural framework and the phase transition.

In Order to investigate the nature of the so-called MPB in $(1 - x)$KNN–xBSC ceramics, XRD patterns of KNN–0.015BSC ceramics were measured at different temperatures. Figure 2 shows the phase structures of KNN–0.015BSC ceramics at different temperatures. According to the characteristic peaks, it can be concluded that the phase structure of KNN–0.015BSC ceramics transforms from the orthorhombic phase to the tetragonal phase then to the cubic phase with increasing measurement temperature. In the XRD patterns of KNN–0.015BSC ceramics show the coexistence of orthorhombic and tetragonal phases at 27, 50, and 80 °C, tetragonal phase at 100, 120, 150, and 200 °C, and cubic phase at 400 °C. This result indicates that the MPB in KNN–0.015BSC ceramics is strongly temperature dependent and the so-called MPB in KNN–0.015BSC ceramics is owing to the formation of the PPT (from the orthorhombic to the tetragonal phase) at room temperature.

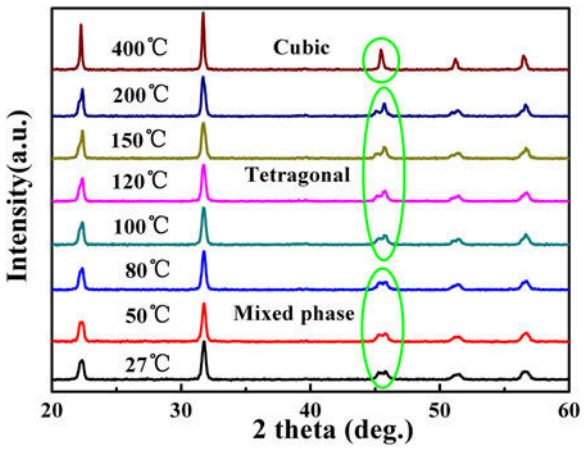

FIG. 2. XRD patterns of KNN–0.015BSC ceramic measured at different temperatures.

Figure 3 shows the SEM micrographs for the $(1 - x)$ KNN–xBSC ceramics. It can be seen from Fig. 3 that quite a number of distinct pores exist in the grain boundary for the ceramics. As the content of BSC increases, the number of pores decreases and the average grain size increases. However, the grain growth cannot eliminate the pores because the morphology of the grains is quadrate. Details of the average grain size G and relative density ρ of the materials studied are summarized in Table I. In addition, all the samples show in general a bimodal grain size distribution for the $(1 - x)$KNN–xBSC ceramics. Average values of grain size increased from ~5 μm for the sample composition, $x = 0.003$ to ~20 μm for the sample composition, $x = 0.025$. That is, most portion of the added BSC facilitates the sintering process and the Co_2O_3 facilitates the grain size increases. The similar phenomenon was observed in the KNN–xCo system.[27]

B. Dielectric properties

The relative permittivity at the frequency of 10 kHz as a function of temperature for the $(1 - x)$KNN–xBSC ceramics can be seen from Fig. 4(a). The $(1 - x)$KNN–xBSC ($x \leq 0.015$) ceramics show two dielectric peaks, which correspond to the phase transitions of T_{O-T} and T_C, respectively. When $x \geq 0.020$, the PPT (at T_{O-T}) disappears and only the cubic–tetragonal phase transition is observed above room temperature. In additional, the dielectric maximum drop down rapidly and the dielectric peaks become extremely broad. This is partially ascribed to the substitution level of BCS is high and the formation of pseudocubic structures. Figure 4(b) plots the T_C and T_{O-T} values of $(1 - x)$KNN–xBSC ceramics as a function of x. Noticeably, the T_{O-T} and T_C decrease with increasing BSC content when $x \leq 0.015$. For pure KNN ceramics, T_{O-T} and T_C are 200 and 420 °C.[29] The T_C shifts from 378 °C for the ceramics ($x = 0.003$) to 360 °C for the ceramics ($x = 0.005$), to 328 °C for the ceramics ($x = 0.010$), and to 321 °C for the ceramics ($x = 0.015$), respectively, while the T_{O-T} was found to shift downward from 197 to 125, to 91 and to 52 °C, significantly expanding the tetragonal phase region. Similar phenomena that both T_C and T_{O-T} of the ceramics move to a lower temperature simultaneously were reported in the KNN–xBA($x = 0$–0.01),[10] KNLNSx–BZ,[19] and KNN–xBNZ[26] ceramics system and the enhancing the properties were found. Figure 4(c) shows the dielectric properties (ε_r and tgδ) values as a function of x for the ceramics. It was found that the ceramics at $x = 0.015$ exhibit a higher dielectric permittivity ($\varepsilon_r = 1494$) and a lower dielectric loss (tgδ = 0.026) at room temperature compared with the other components

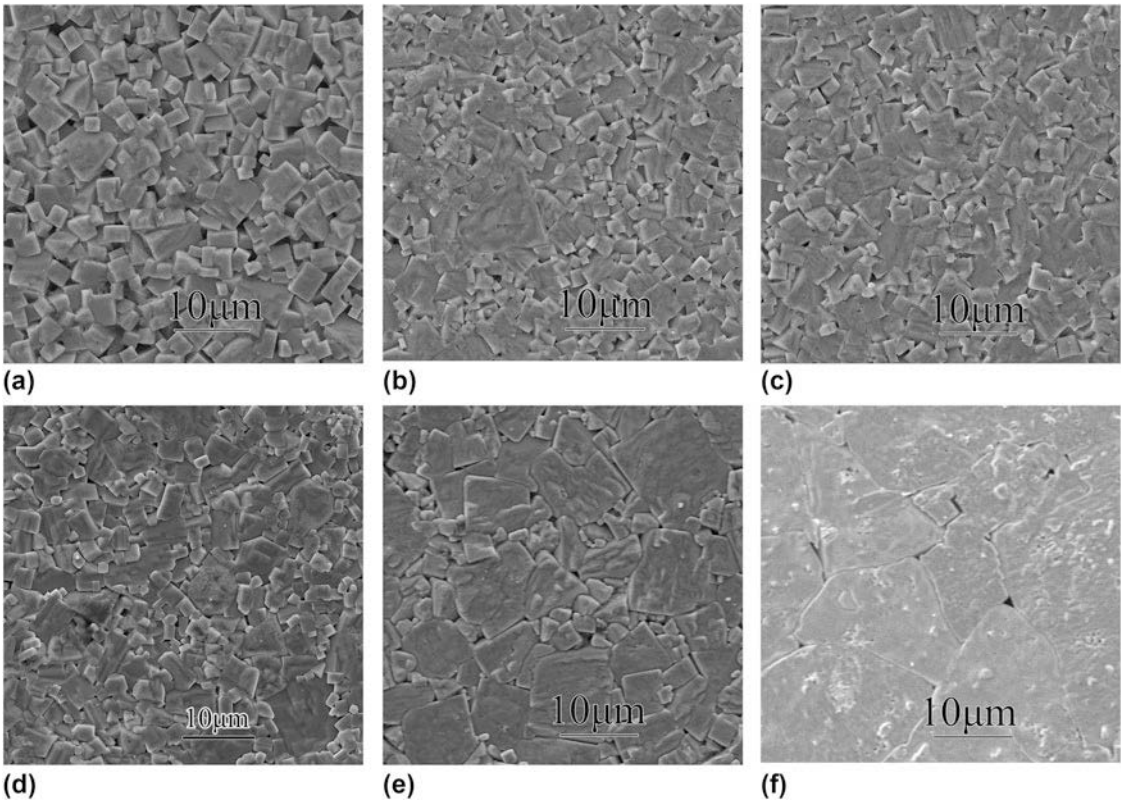

FIG. 3. SEM micrographs of the $(1 - x)$KNN–xBSC ceramics: (a) $x = 0.003$, (b) $x = 0.005$, (c) $x = 0.010$, (d) $x = 0.015$, (e) $x = 0.020$, and (f) $x = 0.025$, respectively.

TABLE I. Summary of parameters of the $(1 - x)$KNN–xBSC ceramics.

BSC content	0.003	0.005	0.010	0.015	0.020	0.025
G (μm)	5.0 ± 1.0	4 ± 0.5	6 ± 1.0	7 ± 1.5	12 ± 2.0	20 ± 4.5
P (g cm^{-3})	4.36	4.39	4.47	4.58	4.58	4.56
T_C (°C)	378	360	328	321	274	250
T_{O-T} (°C)	197	125	91	52	...	...
ε_r (*RT*, 10 kHz)	552	975	1033	1494	1523	1370
tan δ (*RT*, 10 kHz)	0.041	0.028	0.027	0.026	0.028	0.027

of the ceramics. This phenomenon may be explained that the high phase purity and the low T_{O-T} result in the improvement of the dielectric properties in the ceramics at $x = 0.015$. KNN–0.015BSC ceramics exhibit very stable temperature dependence of dielectric permittivity on the order of 1500 from 50 to 300 °C, which demonstrates that KNN–0.015BSC ceramics have important engineering application values.

Figure 5 highlights the variation of the dielectric permittivity (ε_r) and dielectric loss (tgδ) versus the frequency. As it can be seen from Fig. 5(a), the ε_r of all synthesized composites decreases with increase in frequency. The dielectric permittivity value obtained for $x = 0.003$ is around 648 at 10^3 Hz and decreased to 568 as the frequency increased to 10^5 Hz. The samples $x = 0.015$ exhibit a dielectric permittivity value of around 1685 at 10^3 Hz and 1496 at 10^5 Hz. This is because at lower frequency, different types of polarizations, such as electronic, ionic, dipolar, and space charge contribute to the dielectric permittivity but some of them cannot follow up the fast variation of the electric field at high frequency and hence the ε_r; decreases. The dispersion of the ε_r observed at low frequency region for all composites can be explained by Maxwell–Wagner polarization theory.[30,31] Figure 5(b) depicts the variation of tgδ with frequency of the KNN–BSC ceramics. It is observed that the tgδ value decreases with the increase in frequency and is almost constant in the frequency range 10^4–10^5 Hz and then starts increasing. At relatively low frequency, tgδ depends strongly on frequency. This is a common feature observed in ferroelectric materials concerned with ionic conductivity.[32] As the frequency increases, the effect of ionic conductivity becomes small, and the tgδ shows weak frequency dependence.[32]

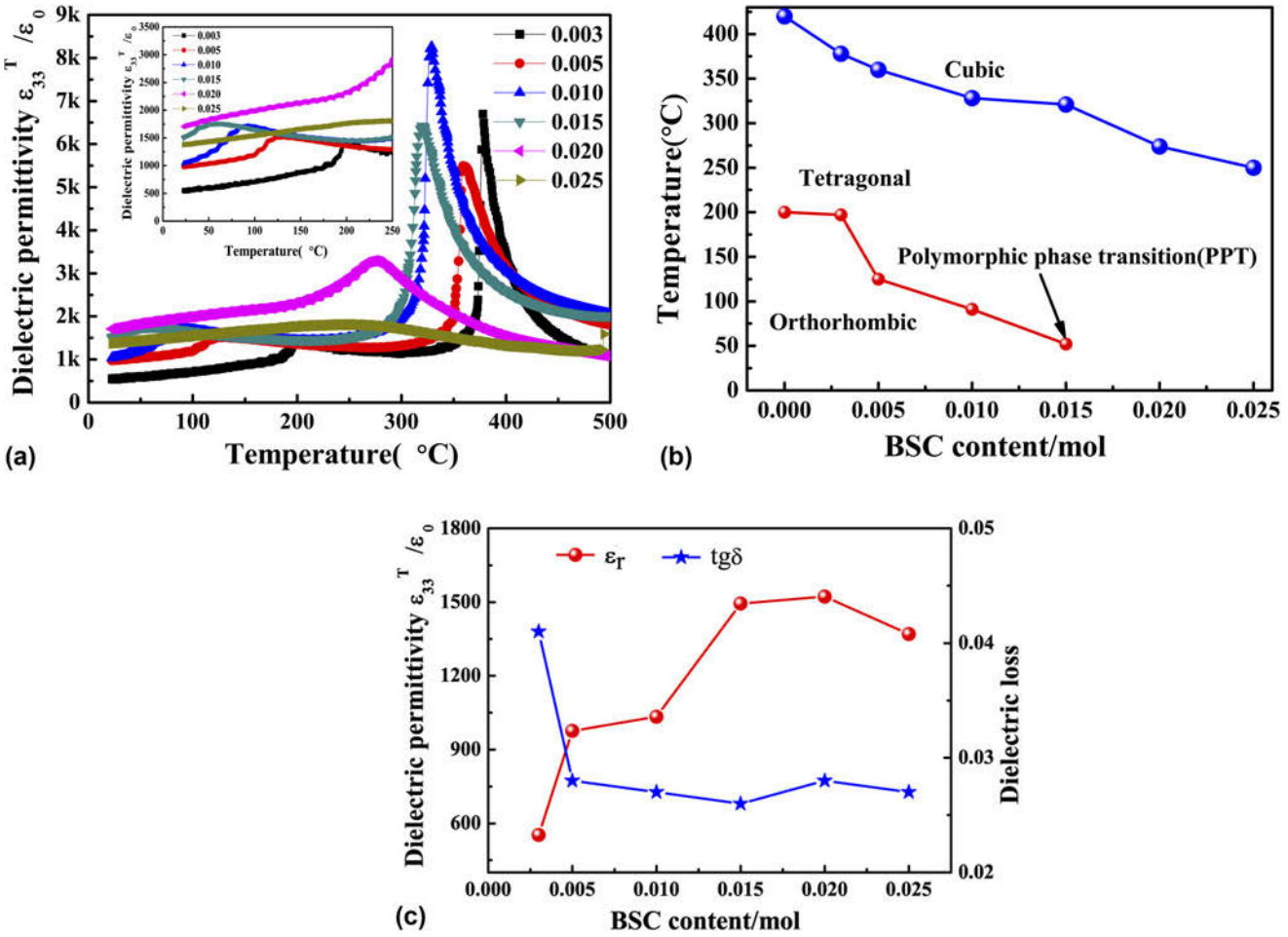

FIG. 4. (a) Temperature dependence of the dielectric properties of $(1-x)$KNN–xBSC ceramics at 10 kHz. (b) Plots of T_C and T_{O-T} values of $(1-x)$KNN–xBSC ceramics as a function of x. (c) The dielectric properties (ε_r and tgδ) values as a function of x for the ceramics at room temperature.

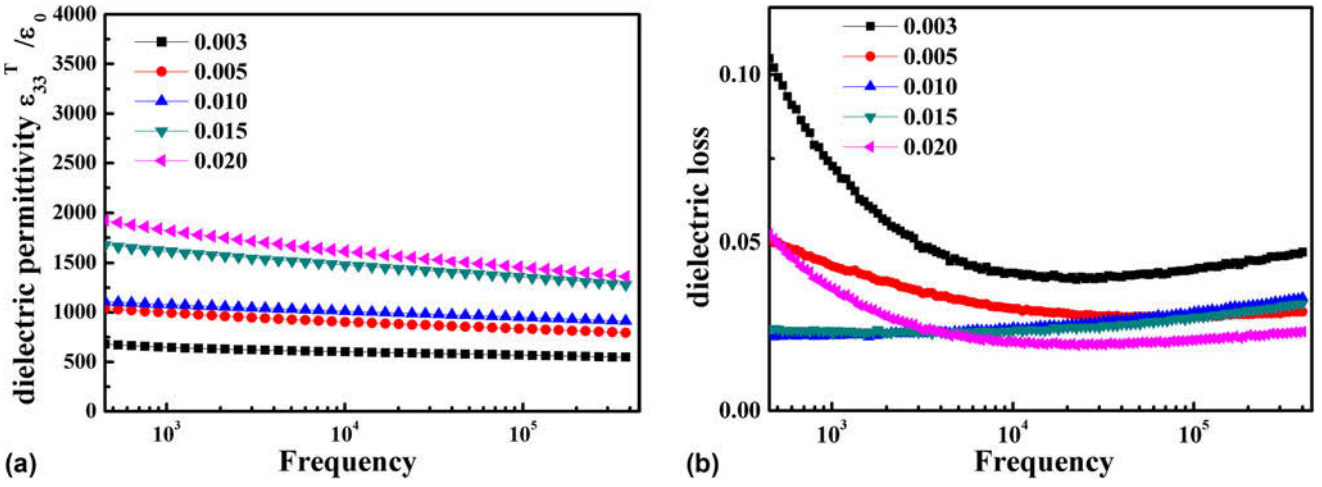

FIG. 5. (a) Dielectric permittivity ε_r and (b) dielectric losses tgδ as function of the frequency for $(1-x)$KNN–xBSC ceramics.

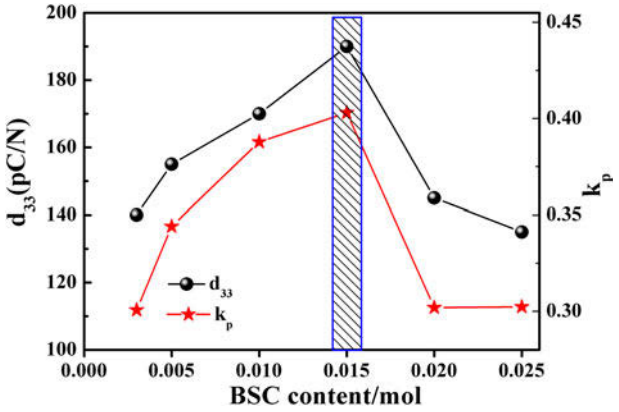

FIG. 6. Values of d_{33} and k_p of $(1 - x)$KNN–xBSC ceramics as a function of x at room temperature.

C. Piezoelectric properties

Figure 6 shows the piezoelectric properties of $(1 - x)$KNN–xBSC ceramics at room temperature. It can be clearly observed that the piezoelectric constant (d_{33}) and the planar electromechanical coupling factor (k_p) of $(1 - x)$KNN–xBSC ceramics firstly increase and then decrease with increasing the BSC content. At $x = 0.015$, the d_{33} and k_p reach their highest values, which are 190 p/CN and 0.403, respectively. In addition, it is also found that the piezoelectric properties of $(1 - x)$KNN–xBSC ceramics are sensitive to the composition; namely, the piezoelectric properties of $(1 - x)$KNN–xBSC ceramics readily decrease when the content of BSC deviates from 0.015. Although the hybridization between Bi-6*p* and O-2*p* orbits can improve the piezoelectric properties of Bi-containing perovskite solid solutions,[15] in this study, the effect is limited and can almost be ignored because the amount of Bi^{3+} additive is too low. KNN–0.015BSC ceramics show high piezoelectric properties should be attributed to: firstly, the dense microstructure caused by doping the optimum BSC content. Secondly, the quantity of the domain wall for the KNN–BSC ceramics decreases because of the increase in the grain size, which makes the domain switch easily, resulting in an optimum piezoelectricity. Moreover, the KNN–0.015BSC ceramics posses both the orthorhombic and tetragonal phases at room temperature, and thus more possible polarization states.

IV. CONCLUSION

Normally sintered $(1 - x)$KNN–xBSC ceramics with high density were obtained. The phase structure and electrical properties of the $(1 - x)$KNN–xBSC system were characterized. XRD analysis revealed the presence of diphasic tetragonal and orthorhombic phases in the ceramics in the vicinity of $x = 0.015$, this coexistence can be ascribed to the formation of a PPT (from the orthorhombic to the tetragonal phase) at room temperature. KNN–0.015BSC ceramics near the PPT possess optimum electrical properties: $d_{33} = 190$ pC/N, $k_p = 40.3\%$, $\varepsilon_r = 1494$, $tg\delta = 0.026$. At the same time, the phase transition temperatures of orthorhombic–tetragonal of the KNN–0.015BSC ceramics are close to room temperature and the Curie temperature T_C is 321 °C. The combination of good piezoelectric properties and high T_C makes these KNN–BSC ceramics suitable for elevated temperature piezoelectric devices.

ACKNOWLEDGMENTS

This work was supported by the National Natural Science Foundation of China (Grant No. 51072165), the fund of State Key Laboratory of Solidification Processing in NWPU (No. KP200901), Doctor Start fund of Baoji University of Arts and Science (ZK15044), the fund of Shaanxi Key Laboratory of Phytochemistry (13JS006) and Shaanxi Provincial Natural Foundation (2013JM6005).

REFERENCES

1. R.C. Turner, P.A. Fuierer, R.E. Newnham, and T.R. Shrout: Materials for high temperature acoustic and vibration sensors: A review. *Appl. Acoust.* **41**, 299 (1994).
2. S. Chen, X.L. Dong, and C.L. Mao: Thermal stability of $(1-x)BiScO_3$-$xPbTiO_3$ piezoelectric ceramics for high-temperature sensor applications. *J. Am. Ceram. Soc.* **89**, 3270 (2006).
3. S.J. Zhang and F.P. Yu: Piezoelectric materials for high temperature sensors. *J. Am. Ceram. Soc.* **94**, 3153 (2011).
4. R.E. Eitel, C.A. Randall, T.R. Shrout, P.W. Rehrig, W. Hackenberger, and S.E. Park: New high temperature morphotropic phase boundary piezoelectrics based on $Bi(Me)O_3$-$PbTiO_3$. *Jpn. J. Appl. Phys.* **40**, 5999 (2001).
5. R.E. Eitel, C.A. Randall, and T.R. Shrout: Preparation and characterization of high temperature perovskite ferroelectrics in the solid solution $(1-x)BiScO_3$-$(x)PbTiO_3$. *Jap. J. Appl. Phys.* **41**, 2099 (2002).
6. S.J. Zhang, C.J. Stringer, R. Xia, S.M. Choi, C.A. Randall, and T.R. Shrout: Investigation of bismuth-based perovskite system: $(1-x)Bi(Ni_{2/3}Nb_{1/3})O_3$-$xPbTiO_3$. *J. Appl. Phys.* **98**, 034103 (2005).
7. S.J. Zhang, R. Xia, C.A. Randall, T.R. Shrout, R.R. Duan, and R.F. Speyer: Dielectric and piezoelectric properties of niobium-modified $BiInO_3$-$PbTiO_3$ perovskite ceramics with high curie temperatures. *J. Mat. Res.* **20**, 2067 (2005).
8. S.M. Choi, C.J. Stringer, T.R. Shrout, and C.A. Randall: Structure and property investigation of a Bi-based perovskite solid solution: $(1-x)Bi(Ni_{1/2}Ti_{1/2})O_3$-$(x)PbTiO_3$. *J. Appl. Phys.* **98**, 34108 (2005).
9. M.H. Jiang, X.Y. Liu, and C.Y. Liu: Effect of $BiFeO_3$ additions on the dielectric and piezoelectric properties of $(K_{0.44}Na_{0.52}Li_{0.04})(Nb_{0.84}Ta_{0.1}Sb_{0.06})O_3$ ceramics. *Mater. Res. Bull.* **45**, 220 (2010).
10. R.Z. Zuo, D.Y. Lv, and J. Fu: Phase transition and electrical properties of lead free $(Na_{0.5}K_{0.5})NbO_3$-$BiAlO_3$ ceramics. *J. Alloy Compd.* **476**, 836 (2009).
11. M.H. Jiang, X.Y. Liu, and G.H. Chen: Dielectric and piezoelectric properties of $BiMnO_3$ doped $0.95Na_{0.5}K_{0.5}NbO_3$-$0.05LiSbO_3$ ceramics. *J. Mater. Sci: Mater. Electron.* **22**, 876 (2011).

12. J.B. Zhao, H.L. Du, and S.B. Qu: The effects of $Bi(Mg_{2/3}Nb_{1/3})O_3$ on piezoelectric and ferroelectric properties of $K_{0.5}Na_{0.5}NbO_3$ lead-free piezoelectric ceramics. *J. Alloys Comp.* **509**, 3537 (2011).
13. H.L. Cheng, H.L. Du, and W.C. Zhou: $Bi(Zn_{2/3}Nb_{1/3})O_3$-$(K_{0.5}Na_{0.5})NbO_3$ high-temperature lead-free ferroelectric ceramics with low capacitance variation in a broad temperature usage range. *J. Am. Ceram. Soc.* **96**, 833 (2013).
14. X.Y. Sun, J. Chen, and R.B. Yu: $BiScO_3$ doped $(Na_{0.5}K_{0.5})NbO_3$ lead-free piezoelectric ceramics. *J. Am. Ceram. Soc.* **92**, 130 (2009).
15. H.L. Du, W.C. Zhou, and F. Luo: Design and electrical properties' investigation of $(K_{0.5}Na_{0.5})NbO_3$-$BiMeO_3$ lead-free piezoelectric ceramics. *J. Appl. Phys.* **104**, 034104 (2008).
16. H.L. Du, W.C. Zhou, and F. Luo: High Tm lead-free relaxor ferroelectrics with broad temperature usage range: $0.04BiScO_3$-$0.96(K_{0.5}Na_{0.5})NbO_3$. *J. Appl. Phys.* **104**, 044104 (2008).
17. W.J. Wu, D.Q. Xiao, and J.G. Wu: Polymorphic phase transition-induced electrical behavior of $BiCoO_3$-modified $(K_{0.48}Na_{0.52})NbO_3$ lead-free piezoelectric ceramics. *J. Alloy Compd.* **509**, L284 (2011).
18. W.J. Wu, D.Q. Xiao, and J.G. Wu: Potassium sodium niobate lead-free piezoelectric materials: Past, present, and future of phase boundaries. *Chem. Rev.* **115**, 2559 (2015).
19. B.Y. Zhang, J.G. Wu, and X.J. Cheng: Lead-free piezoelectrics based on potassium-sodium niobate with giant d_{33}. *ACS Appl. Mater. Interfaces* **5**, 7718 (2013).
20. X.P. Wang, J.G. Wu, and D.Q. Xiao: Giant piezoelectricity in potassium-sodium niobate lead-free ceramics. *J. Am. Chem. Soc.* **136**, 2905 (2014).
21. X.P. Wang, J.G. Wu, and D.Q. Xiao: Large d_{33} in $(K,Na)(Nb,Ta,Sb)O_3$-$(Bi,Na,K)ZrO_3$ lead-free ceramics. *J. Mater. Chem. A* **2**, 4122 (2014).
22. W.F. Liang, W.J. Wu, and D.Q. Xiao: Construction of new morphotropic phase boundary in $0.94(K_{0.42-x}Na_{0.6}Ba_xNb_{1-x}Zr_x)O_3$-$0.06LiSbO_3$ lead-free piezoelectric ceramics. *J. Mater. Sci.* **46**, 6871 (2011).
23. R.P. Wang, H. Bando, and T. Katsumata: Tuning the orthorhombic-rhombohedral phase transition temperature in sodium potassium niobate by incorporating barium zirconate. *Phys. Status Solidi RRL* **3**, 142 (2009).
24. R.Z. Zuo, J. Fu, D.Y. Lv, and Y. Liu: Antimony tuned rhombohdral-orthorhombic phase transition and enhanced piezoelectric properties in sodium potassium niobate. *J. Am. Ceram. Soc.* **93**, 2783 (2010).
25. X.P. Wang, J.G. Wu, and D.Q. Xiao: New potassium-sodium niobate ceramics with a giant d_{33}. *ACS Appl. Mater. Interfaces* **6**, 6177 (2014).
26. Z. Wang, D.Q. Xiao, and G.J. Wu: New lead-free $(1-x)(K_{0.5}Na_{0.5})NbO_3$-$x(Bi_{0.5}Na_{0.5})ZrO_3$ ceramics with high piezoelectricity. *J. Am. Ceram. Soc.* **97**, 688 (2014).
27. G.Z. Zang, X.J. Yi, J. Du, and Y.F. Wang: Co_2O_3 doped $(Na_{0.65}K_{0.35})NbO_3$ piezoceramics. *Mater. Lett.* **64**, 1394 (2010).
28. W.J. Wu, D.Q. Xiao, and J.G. Wu: Piezoelectric properties of $(K_{0.474}Na_{0.474}Li_{0.052})(Nb_{0.948}Sb_{0.052})O_3$-$Co_2O_3$ lead-free ceramics. *J. Ceram. Soc. Jpn.* **119**, 654 (2011).
29. H.L. Du, W.C. Zhou, and F. Luo: Phase structure, dielectric properties, and relaxor behavior of $(K_{0.5}Na_{0.5})NbO_3$-$(Ba_{0.5}Sr_{0.5})TiO_3$ lead-free solid solution for high temperature applications. *J. Appl. Phys.* **105**, 124104 (2009).
30. J.C. Maxwell: *Electricity and Magnetism* (Oxford University Press, London, 1973).
31. K.W. Wagner: Delectric relaxation in distributed dielectric layers. *Ann. Phys.* **40**, 817 (1913).
32. F.R. Marcos, J.J. Romero, and M.G. Navarro: Effect of ZnO on the structure, microstructure and electrical properties of KNN-modified piezoceramics. *J. Eur. Ceram. Soc.* **29**, 3045 (2009).